The Astrophysical Journal, 700:1768–1778, 2009 August 1 doi:10.1088/0004-637X/700/2/1768

HORIZONTAL BRANCH MORPHOLOGY OF GLOBULAR CLUSTERS: A MULTIVARIATE STATISTICAL ANALYSIS

G. Jogesh Babu[1], Tanuka Chattopadhyay[2], Asis Kumar Chattopadhyay[3], and Saptarshi Mondal[3]
[1] The Pennsylvania State University, 326 Thomas Building, University Park, PA 16802-2111, USA; babu@stat.psu.edu
[2] Department of Applied Mathematics, Calcutta University, 92 A.P.C. Road, Calcutta 700009, India; tanuka@iucaa.ernet.in
[3] Department of Statistics, University of Calcutta, 35, B.C. Road, Calcutta 700 019, India; asis_stat@yahoo.com
Received 2008 November 30; accepted 2009 June 4; published 2009 July 16

ABSTRACT

The proper interpretation of horizontal branch (HB) morphology is crucial to the understanding of the formation history of stellar populations. In the present study a multivariate analysis is used (principal component analysis) for the selection of appropriate HB morphology parameter, which, in our case, is the logarithm of effective temperature extent of the HB ($\log T_{\rm eff\,HB}$). Then this parameter is expressed in terms of the most significant observed independent parameters of Galactic globular clusters (GGCs) separately for coherent groups, obtained in a previous work, through a stepwise multiple regression technique. It is found that, metallicity ([Fe/H]), central surface brightness (μ_v), and core radius (r_c) are the significant parameters to explain most of the variations in HB morphology (multiple $R^2 \sim 0.86$) for GGC elonging to the bulge/disk while metallicity ([Fe/H]) and absolute magnitude (M_v) are responsible for GGC belonging to the inner halo (multiple $R^2 \sim 0.52$). The robustness is tested by taking 1000 bootstrap samples. A cluster analysis is performed for the red giant branch (RGB) stars of the GGC belonging to Galactic inner halo (Cluster 2). A multi-episodic star formation is preferred for RGB stars of GGC belonging to this group. It supports the asymptotic giant branch (AGB) model in three episodes instead of two as suggested by Carretta et al. for halo GGC while AGB model is suggested to be revisited for bulge/disk GGC.

Key words: globular clusters: general – methods: statistical

Online-only material: color figures

1. INTRODUCTION

In color–magnitude diagram (CMD) of globular clusters (GCs), horizontal branch (HB) is composed of stars with helium-burning cores and hydrogen-burning shells which have evolved off the red giant branch (RGB). Previous studies have revealed that the variation in the HB morphology is due to metallicity of the cluster. HB stars of the higher metallicity are redder than those of lower metallicity as a result of higher opacity in their envelopes. But metallicity variation is not sufficient to explain in many cases the observed differences between the HB of Galactic globular cluster (GGC), e.g., clusters M2 and M3 have similar metallicities [Fe/H] ~ -1.6 but their HB morphologies are different (Stetson et al. 1996). M2 has a blue HB exhibiting a long tail and M3 on the other hand has comparable number of stars on each side of the RR Lyrae gap. Since HB stars have evolved off the RGB, the corresponding RGB stars have been observed by many authors (Carretta et al. 2006, 2007a, 2007b; Gratton et al. 2001, 2003, 2006). They have found Na–O anticorrelation in these stars having similar metallicities.

These inhomogeneities in the chemical composition of RGB stars have been explained to have primordial origin. The "self-pollution" has been identified as the matter lost in winds of low velocity from asymptotic giant branch (AGB) stars, especially of high mass, evolving during the first phase of life of the clusters and cycling their envelope material through hot CNO cycle at the bottom of their convective envelopes (hot bottom burning (HBB)). Hence, HB stars should be a mixture of two populations. The first one, born together with the intermediate mass population and having the initial helium content and a second additional population more or less enriched in helium formed from the AGB ejecta of the first-generation massive mass stars. Now for models with high helium, the isochrone location is not very sensitive to variations in Y. But for all isochrones there is a small but significant differences in evolving mass: the most relevant feature is that the mass is smaller for larger helium content. The mass differs by 0.05 $M_\odot$ for a difference in helium by 0.04. This difference is important for effective temperature distribution on the HB. In fact if mass loss operates on these two stellar populations then the final stellar mass of helium enriched stars in HB will be several hundredths of solar mass smaller and therefore will have a bluer location (D'Antona et al. 2003; D'Antona & Caloi 2004). Now it is well known that there are two cycles p–p and CNO occur in the stellar interior through which a star converts its material in the core from H to He. So O depletion is accompanied by He enrichment. Now for the first time Carretta et al. (2006) found Na–O anticorrelation while observing the red giant stars in NGC2808 GC. This is explained as a sign of the presence of material processed through the complete CNO cycle where $22_{\rm Ne}$ is transformed to $23_{\rm Na}$ by proton capture at that temperature (Denisenkov & Denisenkova 1989; Langer et al. 1993). Hence, enhanced Na abundances should accompany O depletion and O depletion accompany He enrichment. So the extended blue tails are directly linked to the enhanced helium (or enhanced Na) in the matter (D'Antona et al. 2003), processed through HBB, from which these stars are born. This interpretation leads to the idea that GC stars are formed in two main generations, the first one formed having the composition of the primordial gas cloud and the second one formed directly from the AGB ejecta of the first massive mass stars over a span of time lasting $\sim 2 \times 10^8$ yr. As a result HB stars play an important role in explaining the formation history of the GGC stars.

There are different measures for describing the morphology of the HB. One way of quantifying this is through the parameter $C = \frac{(B-R)}{B+V+R}$ (Zinn 1986; Lee 1990) where B is the number of

stars on the blue side of the RR Lyrae gap, R is the number of stars on the red side, and V is the number of RR Lyrae variable stars on HB. The other measures are HB_{RE}, defined as the intrinsic $(B-V)_0$ color of the point adopted on the basis of estimation of the red endpoint of the observed HB, L_t, defined as the total length of the HB measured from HB_{RE} down to the blue end of the HB, $(B-V)_{peak}$, measured by dividing the whole length into bins starting from HB_{RE} and counting the stars populating each bin perpendicular to the adopted ridge line, BT, defined as the length of the blue tail measured along the ridge line of the HB starting from $(B-V)_{peak}$ down to the adopted blue HB extreme and Dickens Type (DT; Fusi Pecci et al. 1993). Sometimes maximum effective temperature along HB is also used as the parameter (Recio-Blanco et al. 2006, hereafter RB06). Different measures are used because in many situations clusters having a similar value of the morphology index actually have significant differences in their HB distributions. For instance (Fusi Pecci et al. 1993), both NGC 6793 and NGC 6752 have HB stars populating only blue side of the instability strip with $C = 1$ in both cases. We observe, star distributions along the blue tail of NGC 6752 is very long with gaps lacking in NGC 6093. The DT measure is much better option in dealing with blue tails. For instance DT = 2 for NGC 6093 while it is 1 for NGC 6752. So it is very important to select first which of the above mentioned parameters is the optimum one which takes into account significant part of variations of GCs. As in the previous literatures it appears that scientists have used different HB parameters to explain the morphology, we have started our study using principal component analysis (PCA) to identify the proper HB morphology parameter.

Once the HB morphology parameter is properly identified it is explained in terms of other observable independent parameters, to understand the different characteristics of the HB stars. As mentioned earlier previous studies have identified metallicity as the first parameter. But in many situations GCs with HBs having similar metallicities may show different natures (Sandage & Wildey 1967; Rood 1973). Therefore, other parameters have been suggested by various authors as possible second parameter besides metallicity. Age has long been regarded as second parameter (Sarajedini et al. 1997; Bolte 1989). For clusters older than 10 Gyr, the core mass of stars on the HB is roughly constant. Thus, variation of the total stellar mass is due to the variation in mass of envelopes of stars. As the age of clusters increases, the mean mass of stars evolving onto the HB decreases and the mass of their envelopes also decreases. Thus, older clusters have HB stars with lower opacity envelopes which are therefore bluer than more massive HB stars in younger clusters. However, Stetson et al. (1996) have carried out an analysis of age differences and this yields smaller age differences between GCs to take into account the sufficient mass loss. Moehler et al. (1999) showed that helium mixing can explain the discrepancies from canonical models for HB stars between 11,500 and 20,000 K. If deep mixing currents extend into the H burning in the RGB, He can be mixed into the stellar envelope. The He enrichment increases the H-burning rate leading to higher luminosity and lower gravity compared with canonical HB stars of same temperature. Carvalho (1999) found Al as another indication of He mixing. Buonanno et al. (1997) performed an extensive analysis of 63 GCs and found that the net length of HB and the presence of an extended vertical blue tail are correlated with cluster density. More concentrated or denser clusters having bluer and longer HB morphologies are interpreted by enhanced mass loss from the HB progenitors in the RGB phase, possibly due to increase in interaction between stars in denser cluster environment. Rotation (Sweigart 1997) and the presence of planets (Soker 1998) are the other possible second parameters.

The above studies are mostly based on data sets involving only a few GCs at a time and the comparison was done on the basis of a single parameter. Dealing with one parameter at a time we are ignoring the combining effects of the remaining ones. To overcome this difficulty RB06 have carried out a multivariate analysis of the HB stars of GGC. They found that more massive clusters tend to have HB's more extended to higher temperatures. For this they have used linear regression using the parameters arising out of PCA giving maximum variations. For linear regression, it is necessary to select the number of independent parameters which are mainly responsible for the total variation in the dependent variable (here HB morphology parameter). While selecting this set of independent parameters they have used PCA to reduce the dimension by considering all the dependent and independent parameters together. When faced with a predictive modeling problem that has many possible predictor effects a natural question is which subset of the effects provides the best model for the data. Statistical model selection seeks to answer this question, employing a variety of definitions of the "best" model as well as a variety of heuristic procedures for approximating the true but computationally infeasible solution. Methods include not only extensions to generalized linear model (GLM)-type models of methods long familiar in the regression procedure (forward, backward, and stepwise) but also the new methods of Tibshirani (1996) and Efron et al. (2004). Statistical packages support a variety of fit statistics that one can specify as criteria for choosing the best model. Among them the following two statistics are available: AIC, the Akaike information criterion (Darlington 1968; Judge et al. 1985), BIC, the Sawa's Bayesian information criterion (Sawa 1978; Judge et al. 1985). In our study, we have used the stepwise regression to identify the optimum set of independent parameters which accounts for variation in HB morphology most clearly. The stepwise method is discussed in Chattopadhyay & Chattopadhyay (2006). RB06 have also considered a single sample consisting of all GGC. Various classification studies of GGC (Zinn 1993; Mackey & Gilmore 2004; Mackey & van den Bergh 2005; Chattopadhyay & Chattopadhyay 2007, hereafter CC07) have shown that there are three populations of GGC. One is bulge/disk GCs, one is inner halo GCs, and the other is outer halo GCs. In the present study, we have taken these samples of GCs following CC07 and applied the stepwise regression technique separately to these coherent groups.

In our study, it is found that different parameter sets are responsible for significant variation of HB morphology in different regions (bulge/disk, inner halo, and outer halo) and the scatter is reduced by a significant amount compared to the previous (RB06) study. We have validated our study by taking several (1000) bootstrap samples.

To study the chemical anomalies of HB stars, we have taken some samples of RGB stars of GGC (Carretta et al. 2006, 2007a, 2007b; Gratton et al. 2006) and have carried out cluster analysis (CA) with respect to chemical abundances (Na and O), color $(B-V)$, and magnitude (V) to identify different groups in RGB stars. We have found three groups instead of two as demonstrated by previous authors (Carretta et al. 2006, 2007a, 2007b) indicating multi-episodic star formation for RGB. So the new aspects of our study are as follows.

Table 1
Correlation Matrix among the 12 Independent Parameters and HB Morphology Parameters of Data Set 1

Parameter	$\log T_{\rm eff\,HB}$	DT	HBR	HB_{RE}	L_t	$(B-V)_{\rm peak}$	BT
[Fe/H]	−0.656(0.0)	0.632(0.0)	−0.764(0.0)	0.698(0.0)	0.110(0.585)	0.766(0.0)	0.223(0.264)
He	0.248(0.109)	−0.304(0.124)	0.396(0.050)	−0.308(0.120)	0.147(0.463)	−0.291(0.140)	0.141(0.484)
M_v	−0.433(0.0)	0.169(0.400)	−0.015(0.940)	−0.040(0.840)	−0.254(0.201)	−0.022(0.914)	−0.306(0.121)
$\Gamma_{\rm col}$	0.123(0.430)	−0.143(0.480)	−0.080(0.700)	0.082(0.680)	0.062(0.757)	−0.090(0.656)	0.140(0.487)
ρ_0	0.158(0.313)	−0.257(0.200)	−0.010(0.960)	0.047(0.820)	0.212(0.289)	−0.036(0.858)	0.201(0.316)
c	0.063(0.687)	−0.315(0.110)	0.133(0.550)	−0.176(0.380)	−0.013(0.947)	−0.206(0.303)	−0.045(0.825)
$R_{\rm gc}$	0.159(0.310)	−0.191(0.340)	0.058(0.780)	−0.294(0.140)	−0.187(0.351)	−0.128(0.524)	−0.129(0.522)
r_h	−0.156(0.320)	0.310(0.120)	−0.094(0.650)	0.198(0.320)	−0.101(0.615)	0.189(0.345)	−0.197(0.325)
$t_{\rm rc}$	0.068(0.660)	0.298(0.130)	−0.106(0.620)	0.100(0.620)	−0.089(0.659)	0.184(0.358)	−0.006(0.975)
$t_{\rm rh}$	0.208(0.180)	0.095(0.640)	0.064(0.760)	−0.059(0.760)	−0.038(0.852)	−0.048(0.811)	−0.082(0.685)
μ_v	−0.274(0.080)	0.207(0.300)	0.030(0.890)	−0.056(0.780)	−0.156(0.438)	−0.033(0.868)	−0.209(0.296)
r_c	−0.041(0.790)	0.248(0.210)	−0.046(0.830)	0.096(0.630)	−0.089(0.660)	0.123(0.540)	−0.067(0.740)

1. We have selected the proper HB morphology parameter in an objective way using PCA (Chattopadhyay & Chattopadhyay 2006).
2. We have taken three subgroups of GGC following CC07 instead of one as taken by RB06.
3. We have applied stepwise multiple regression technique instead of ordinary regression used by RB06.
4. We have applied a CA (CC07) technique to the different samples of RGB stars of GGC to verify the actual number of subpopulations and compared them to the previous results. A change point analysis (discussed in the Appendix) has also been carried out to verify the nature of different subgroups of GGC obtained by CA.

In Section 2, the data used are discussed. In Section 3, the optimum selection of HB morphology parameter has been carried out. In Section 4, the stepwise regression is applied to three groups of GGC and using several bootstrap samples generated from the original samples the regression coefficients are estimated. In Section 5, the CA is carried out for different RGB stars of GGC and the different classes are discussed in light of the "self-pollution" model. Conclusions are elucidated in Section 6.

2. DATA SET

Our analysis is based on four data sets of GCs in Milky Way which have appropriate photometric and structural parameter values.

Data set 1. This consists of 50 GCs taken from RB06. The parameters used for study are HB morphology parameter ($\log T_{\rm eff\,HB}$), absolute visual magnitude (M_v), concentration parameter (c), distance from the Galactic center ($R_{\rm gc}$) in Kpc, logarithm of core relaxation time in year ($t_{\rm rh}$), core radius (r_c) in parsecs, central surface brightness (μ_v) per square arcseconds, metallicity ([Fe/H]), collision parameter ($\Gamma_{\rm col}$), central luminosity density (ρ_0), half-light radius (r_h) in parsec, core relaxation time ($t_{\rm rc}$; RB06), initial helium abundance (He; Salaris et al. 2004), and HB morphology parameters HBR, HB_{RE}, DT, L_t, BT, $(B-V)_{\rm peak}$ (Fusi Pecci et al. 1993).

Data set 2. This consists of 94 red giant stars in the GGC NGC 2808 (Carretta et al. 2006). The parameters used for study are V, $B-V$, [Na/Fe], and [O/Fe].

Data set 3. This consists of 137 red giant stars in the GGC NGC 6752 (Carretta et al. 2007a). The parameters used for study are V, $B-V$, [Na/Fe], and [O/Fe], respectively.

Data set 4. This consists of 79 red giant stars in the GGC NGC 6218 (Carretta et al. 2007b). The parameters used for study are V, $B-V$, [Na/Fe], and [O/Fe], respectively.

Table 2
Correlation Matrix among the HB Morphology Parameters of Data Set 1

Parameter	DT	HBR	HB_{RE}	L_t	$(B-V)_{\rm peak}$	BT	$\log T_{\rm eff\,HB}$
DT	1						
HBR	−0.77	1					
HB_{RE}	0.69	−0.89	1				
L_t	−0.24	−0.002	0.22	1			
$(B-V)_{\rm peak}$	0.69	−0.94	0.86	0.022	1		
BT	−0.20	−0.12	0.24	0.93	0.19	1	
$\log T_{\rm eff\,HB}$	−0.70	0.57	−0.42	0.61	−0.52	0.60	1

3. SELECTION OF PROPER HB MORPHOLOGY PARAMETER

In order to select the appropriate HB morphology parameter, we have first computed the correlation of 12 available independent parameters viz. [Fe/H], M_v, c, $R_{\rm gc}$, $t_{\rm rh}$, r_c, μ_v, He, $\Gamma_{\rm col}$, ρ_0, r_h, $t_{\rm rc}$ with the HB morphology parameters $\log T_{\rm eff\,HB}$, DT, HBR, HB_{RE}, L_t, $(B-V)_{\rm peak}$, and BT (Data set 1). Table 1 shows the correlation values along with their p values (within parenthesis) corresponding to the test for zero correlation. From the p values, it can be inferred that the parameters like L_t, $(B-V)_{\rm peak}$, BT are uncorrelated with almost all the independent parameters. DT, HBR, $(B-V)_{\rm peak}$ and HB_{RE} have significant correlations (p value <0.05) only with [Fe/H] while $\log T_{\rm eff\,HB}$ has strong correlation with both [Fe/H] and M_v. In previous works also authors claimed that [Fe/H] and M_v are important independent parameters. As such $\log T_{\rm eff\,HB}$ may be considered as a prominent dependent parameter to study HB morphology explained by [Fe/H] and M_v. While studying the correlation matrix (Table 2) of the HB morphology parameters, namely, DT, HBR, HB_{RE}, L_t, $(B-V)_{\rm peak}$, BT, $\log T_{\rm eff\,HB}$ (Data set 1) we see that only $\log T_{\rm eff\,HB}$ has good correlations with most of the other HB parameters.

Depending upon the above computation $\log T_{\rm eff\,HB}$ may be considered as a good HB morphology parameter since it may replace most of the other parameters because of its strong correlations. In order to establish the above phenomenon through appropriate multivariate analysis we have also applied PCA. Using PCA (Chattopadhyay & Chattopadhyay 2006, hereafter CC06), we see that if we take HBR, HB_{RE}, DT, L_t, BT, and $(B-V)_{\rm peak}$ by excluding $\log T_{\rm eff\,HB}$ from the set then in the first component there are HBR, HB_{RE}, DT, $(B-V)_{\rm peak}$ while in second component there are L_t and BT (Table 3 and Figure 1). Here, Figures 1–4 are the biplots (correlation vector diagrams) corresponding to PCA.

Table 3
PCA for the HB Morphology Parameters for Data Set 1

Set	Principal Component	Eigen Value	Cumulative %
S1 (DT, HBR, HB_{RE}, L_t, $(B-V)_{peak}$, BT)	1	1.9	57.47
	2	1.4	91.51
	3	0.5	96.27
	4	0.4	98.96
	5	0.2	99.72
	6	0.1	100.00
S2 (HBR, L_t, [Fe/H])	1	1.3	58.89
	2	1.0	92.21
	3	0.5	100.0
S3 (HBR, L_t, M_v)	1	1.1	41.81
	2	1.0	75.16
	3	0.9	100.0
S4 (HBR, L_t, [Fe/H], M_v, log $T_{eff\,HB}$)	1	1.5	46.27
	2	1.3	77.57
	3	0.9	92.59
	4	0.5	97.76
	5	0.3	100.00

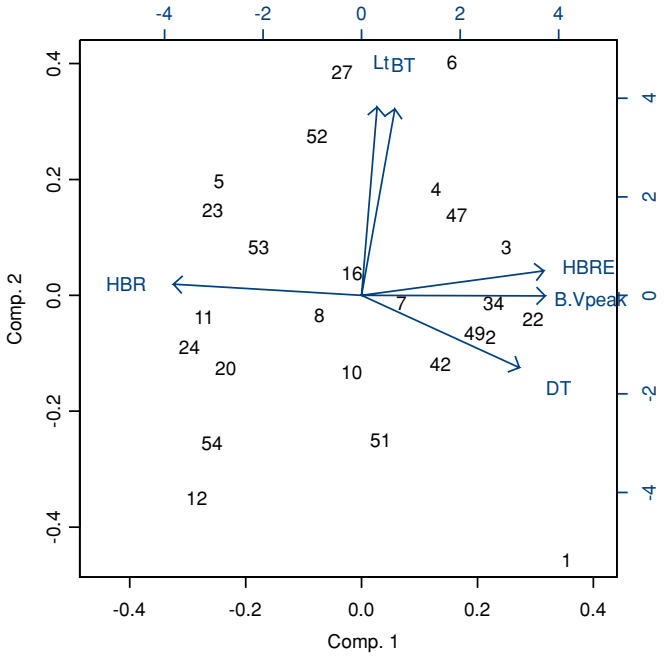

Figure 1. PCA for the HB morphology parameters HBR, HB_{RE}, DT, L_t, BT, and $(B-V)_{peak}$ of Data set 1.

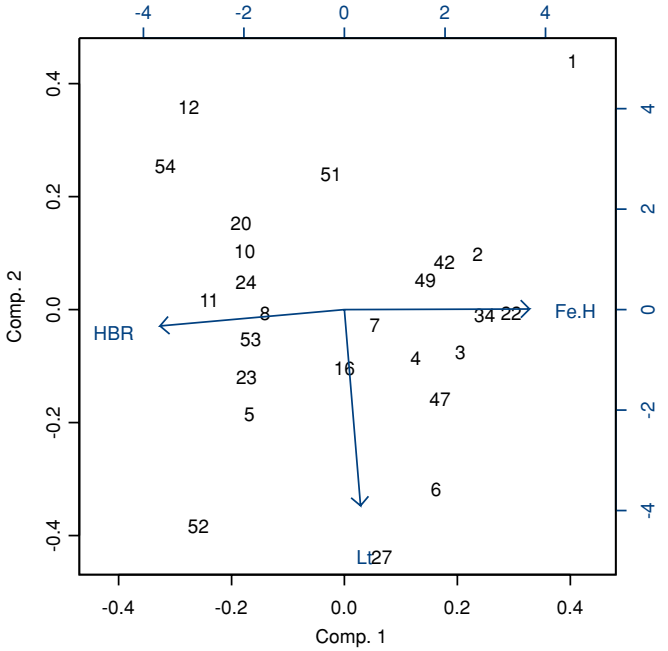

Figure 2. PCA for the HB morphology parameters HBR, [Fe/H], and L_t of Data set 1.

At the second step we have chosen two representative morphological parameters from the two components, namely, HBR and L_t and studied their variations with respect to independent parameters [Fe/H] and M_v. Initially, we have chosen these two independent parameters because of the reasons discussed above regarding Table 1. Latter, we have included more independent parameters (12) through stepwise multiple regression technique for a better prediction of the morphology parameter (Section 4). First, we have taken HBR, L_t, and [Fe/H] (Figure 2). Here, PCA shows that [Fe/H] belongs to the same component with HBR. Then we have taken HBR, L_t, and M_v. PCA shows that M_v is in the same component with L_t (Figure 3). From this it may be inferred that the choice of HBR is not sensitive to variation in M_v while choice of L_t is not sensitive to variation in [Fe/H] values. Finally, we have chosen L_t, HBR, [Fe/H], M_v, and log $T_{eff\,HB}$ together and here from PCA it appears that log $T_{eff\,HB}$ has contribution to two different components of which in one component there is [Fe/H] and in the other there is M_v (Figure 4). Thus, as a result log $T_{eff\,HB}$ seems to be sensitive to both of the independent parameters [Fe/H] and M_v. Hence, it may be concluded that log $T_{eff\,HB}$ may be selected as the proper HB morphology parameter for comparison.

4. CLUSTER ANALYSIS AND MULTIPLE REGRESSION

CC07 have carried out an objective classification of the GGC. In that work a PCA is performed to search for the optimum set of parameters giving the maximum over all variation among the GCs in Milky Way. It is found that metallicity, concentration, and core radius are the parameters responsible for maximum variation in the GCs of Milky Way. Under the multivariate set up since various parameters are responsible for the variation among

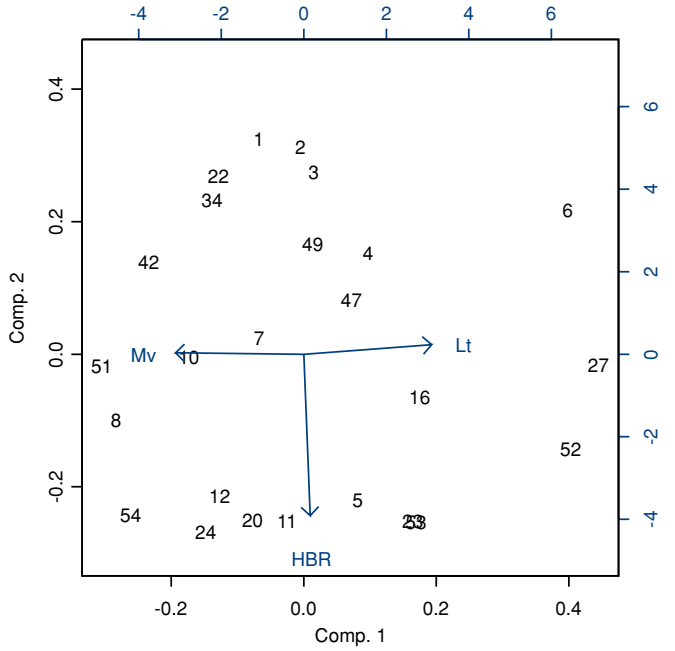

Figure 3. PCA for the HB morphology parameters HBR, M_v, and L_t of Data set 1.

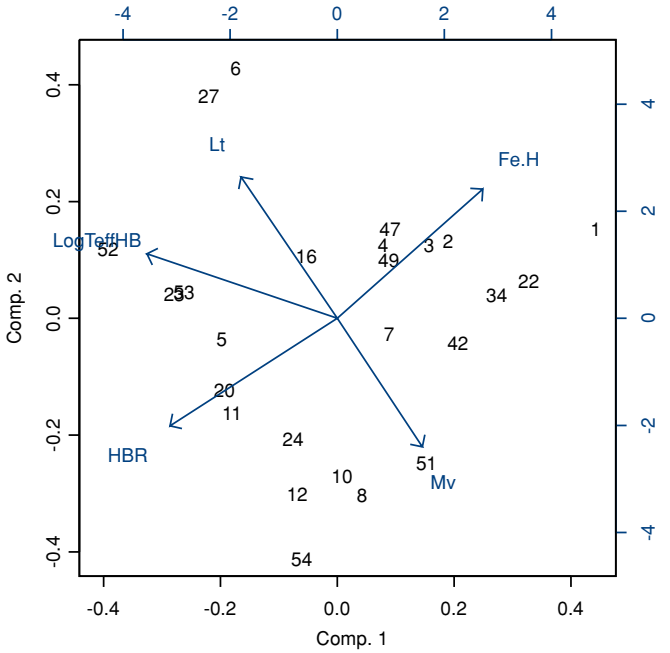

Figure 4. PCA for the HB morphology parameters L_t, HBR, [Fe/H], M_v, and $\log T_{\rm eff\,HB}$ of Data set 1.

GCs, it is better to select the optimum set giving maximum variation. This is the goal of PCA. Then a classification is carried out with respect to this optimum set of parameters applying CA technique. Here, partitioning method constructing K classes is used (MacQueen 1967) and the optimum value of K found is 3 (Sugar & James 2003). They have also studied the kinematics of these subgroups. GCs of Cluster 1 have high metallicities, very low core radii, high rotational velocity and are close to the center of the Galaxy. GCs of Cluster 2 have minimum metallicity, small rotation, far from Galactic disk and have moderate core radii. The GCs of the remaining group (Cluster 3) have high core radii, small rotation, highest velocity dispersion and are farthest from the Galactic center. Thus, these groups are associated with bulge/disk, inner halo and outer halo of the Galaxy, respectively. Hence, we have carried out CA with the present sample (Data set 1) taking $K = 3$ and applied a stepwise multiple regression technique (CC06) taking $\log T_{\rm eff\,HB}$ as a predicted variable (found in the analysis of Section 3) separately to these three groups emerging out of the analysis. The CA is carried out with respect to a set of independent parameters M_v, c, $R_{\rm GC}$, $t_{\rm rc}$, r_c, μ_v, [Fe/H], and He which are selected from a set of 12 parameters (the above eight and collision parameter $\Gamma_{\rm col}$, central luminosity density ρ_0, half-light radius r_h, relaxation time at half-light radius $t_{\rm rh}$ of RB06 by examining the pairwise scatter diagrams (Figures 5 and 6)).

Figure 6 indicates that all the eight independent parameters selected for CA are quite uncorrelated with a good extent while the remaining ones are in some way correlated with these eight parameters (Figure 5). From Figure 6, it also appears that with respect to correlations among different parameters there is clustering nature in the data. For example in the cells corresponding to c against μ_v and r_c against $R_{\rm GC}$, the presence of cluster effect is very clear. The parameter $\rm Age_{rel}$, (RB06) which indicates the relative ages of the GGC is not selected for the following reasons. (1) Many values are missing (seven out of 50 GGC) which exceeds 5% of the total sample size. (2) As we have already mentioned that "age" has played a controversial part in solving "second parameter" problem so exclusion of that parameter may affect the final result. But while doing the CA (with reduced data set of size 43) we found that when age is included in the set of clustering parameters the result we get remains almost the same when we have excluded it in the sample of larger size ($\sim$50) under consideration. Also there are controversial opinions of different authors regarding consideration of age as second parameter. According to Sarajedini et al. (1997) the age of clusters in the Galaxy varies by 2–4 Gyr. For example, two GCs NGC362 and NGC288 have similar metallicity ([Fe/H] ~ -1.3) but HB stars in NGC362 form a red clump whereas NGC288 showed that main-sequence turn-off for NGC362 is brighter than for NGC288. From this he concluded that NGC362 is younger by an age of about 3 Gyr. In the work Stetson et al. (1996) analyzed the whole picture again using NGC1851 as a bridge between NGC288 and NGC362 and found that there is not any significant age difference between the clusters. Considering all the above facts we have not included "age" in our data set.

The CA shows that there are 24 GCs in Cluster 1, 18 GCs in Cluster 2, and eight GCs in Cluster 3. On the basis of the CA for the present sample with respect to a larger set of parameters compared to CC07, it is found that the trend in Cluster mean values (Table 7) almost remains the same for the observed parameters except for r_c which may be due to the fact that the GCs considered in the present sample are compact in nature. Regarding the membership of the GCs it is found that in Cluster 1, it remains exactly the same and if we combine Clusters 2 and 3 we get almost similar result with around 7% misclassification. Due to less number of GCs in the present situation Cluster 3 separately is somewhat different from the previous situation (CC07) but it does not affect the final result as most of the studies are based on Cluster 1 and Cluster 2. Finally, the regression technique is applied to Clusters 1 and 2 separately for the prediction of $\log T_{\rm eff\,HB}$. These are

$$\log T_{\rm eff\,HB} = 6.0514 - 0.4102[{\rm Fe/H}] - 0.1510\mu_v - 0.1258r_c \quad (1)$$

with p value 0.00, rms = 0.10, and multiple $R^2 = 0.8574$ for

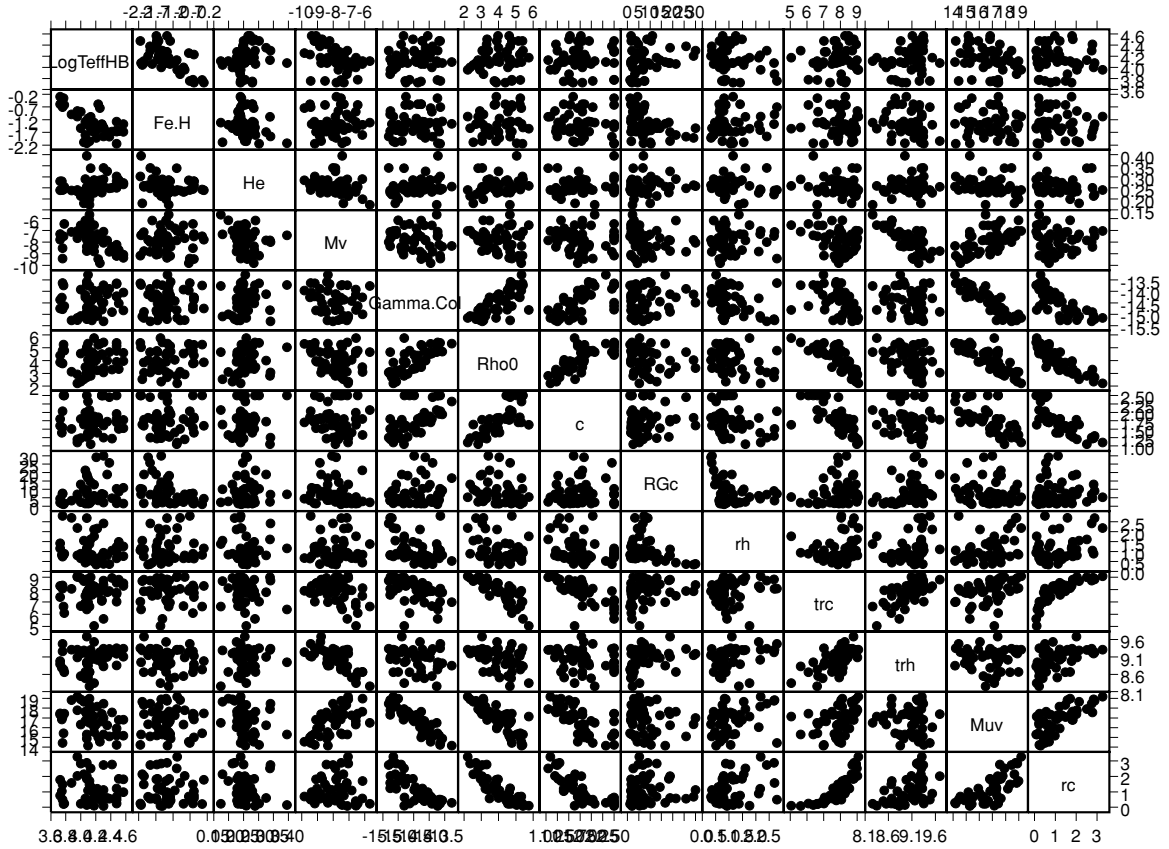

Figure 5. Pairwise scatter diagrams of the 13 parameters of Data set 1.

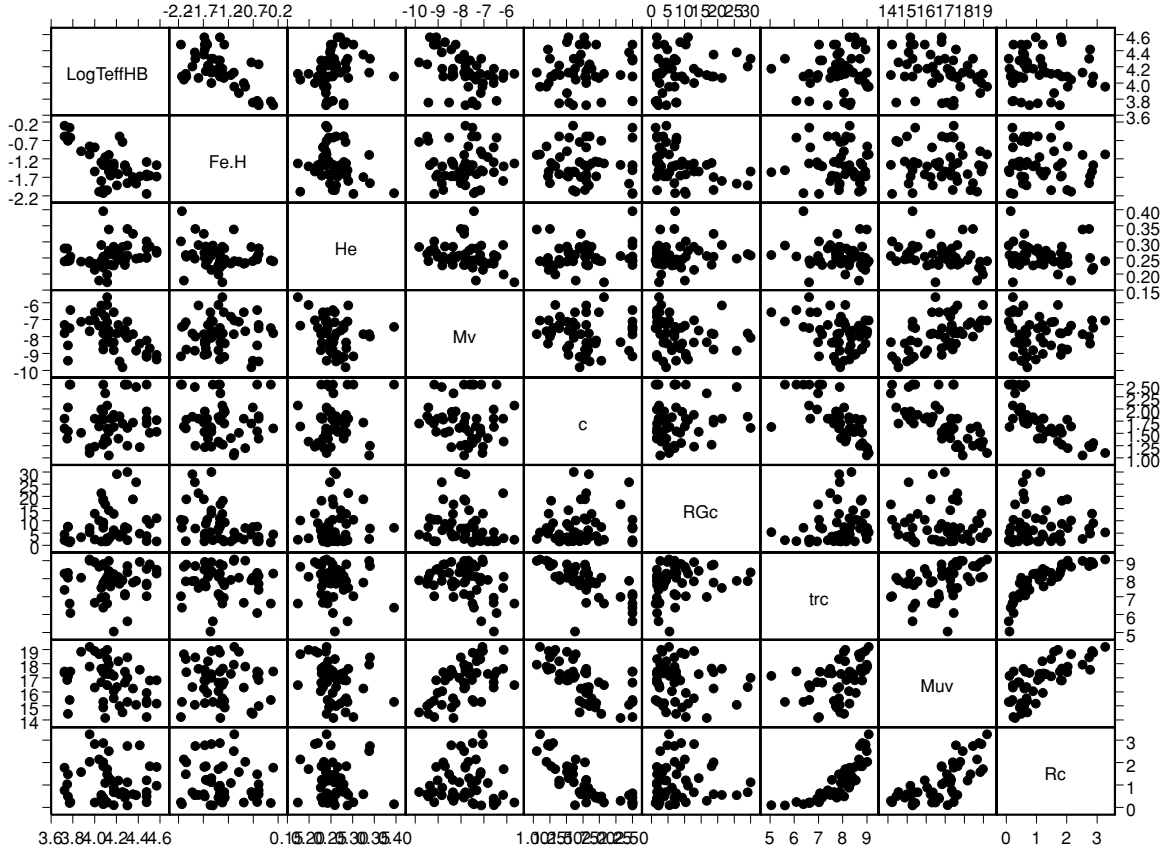

Figure 6. Pairwise scatter diagrams of the selected eight independent and horizontal morphology parameters of Data set 1.

Cluster 1 and

$$\log T_{\rm eff\,HB} = 2.3951 - 0.3596[{\rm Fe/H}] - 0.1525 M_v \quad (2)$$

with p value 0.00, rms = 0.17, and multiple $R^2 = 0.5207$ for Cluster 2, respectively.

Since the total number of parameters is equal to the number of members in Cluster 3 this technique is not applicable for Cluster 3. On the other hand, we have combined GGC of Clusters 2 and 3 (as both are halo members) and applied the technique to the combined group and the relation found is

$$\log T_{\rm eff\,HB} = 2.7903 - 0.2997[{\rm Fe/H}] - 0.1144 M_v. \quad (3)$$

Since the above relation is similar to Equation (2), we have applied ordinary regression to the parameter set ($\log T_{\rm eff\,HB}$, [Fe/H], and M_v) to the GGC of Cluster 3 and the relation found is

$$\log T_{\rm eff\,HB} = 3.63 - 0.067[{\rm Fe/H}] - 0.0569 M_v \quad (4)$$

with p value 0.66, $R^2 = 0.15$, and rms = 0.15.

To test the robustness of the above relations we have taken 1000 bootstrap samples and estimated the coefficients which are given in Tables 4–6 for Clusters 1–3, respectively. It is clear from the tables that all the values estimated are consistent with the values found with the original sample with a very small bias and small variance.

It is also clear from Equation (1) that for bulge/disk GCs, the morphological parameter is mainly determined by the chemical composition and the cluster environment, i.e., compactness of the cluster. The fit is much better (multiple $R^2 \sim 0.8574$) than found by RB06 (multiple $R^2 \sim 0.5256$) considering the whole sample of GGC at a time. Fusi Pecci et al. (1993) found that the extent of blue tail of the HB is correlated with cluster density and concentration, i.e., more concentrated or denser clusters have bluer and longer HB morphologies. This is interpreted as enhanced mass removal from HB progenitors possibly due to increase of interactions between stars in denser cluster environment. Thus, cluster environment can affect the stellar evolution leading to HB morphology. On the other hand the extended blue tails of HB are interpreted in terms of a second generation of stars born from the ejecta of the AGB stars of the first stellar generation. The most common hypothesis for the origin of chemical peculiarities are either (1) deep mixing in cluster members of material nuclearly processed in their interior or (2) pollution by external material. As a result of deep mixing blue HB can form (Langer & Hoffman 1995; Sweigart 1997) but extremely blue tail requires extreme mass loss (larger than 0.01 $M_\odot$) which is not possible by deep mixing in the envelopes of red giants (Caloi 2001). On the other hand, D'Antona et al. (2003) showed that the morphology of HB is affected by a helium variation. They found that isochrone with initial helium content $Y = 0.28$ reaches the red giant tip with a mass of 0.05 $M_\odot$ smaller than in case with standard helium ($Y = 0.24$). They also carried out simulations with two components, one with $Z = 0.001$ and $Y = 0.24$ and other with initial helium content between $Y = 0.24$ and $Y = 0.28$. They assumed mass-loss law following Reimers (1977), i.e., more mass is lost on average from helium-rich (smaller mass) evolving giants. It is found that He-rich populations occupy the blue tail while standard He stars occupy red part of HB (Figure 4; D'Antona et al. 2003) showing two subpopulations with different He content. If it is so then there must be helium discontinuity between two subgroups of HB stars. In fact the AGB ejecta from which the second generation is born are all helium enriched (D'Antona et al. 2003) and these stars have bluer location along HB with respect to first-generation intermediate mass HB stars. This model successfully explained HB of NGC 2808 (D'Antona & Caloi 2004). Now He enrichment means O depletion and Na enrichment. So there should be Na–O anticorrelation in the AGB stars. Observations (Carretta et al. 2006; Gratton et al. 2006) have confirmed Na–O anticorrelation for RGB stars in these clusters. But AGB model cannot predict a very high helium abundance (∼0.4) which is found for blue HB stars in cluster $\omega_{\rm Cen}$ (Norris 2004; Piotto et al. 2005) and NGC 2808 (D'Antona et al. 2005). The maximum value computed is $Y = 0.36$ (Lattanzio et al. 2004). A third episode of star formation has been suggested (Ventura & D'Antona 2005), but too many episodes do not preserve the constancy of C+N+O, though some observations have been found for three groups of HB stars (Castellani et al. 2006; Catelan et al. 2002). Recently, multiband observations of the GGC NGC 6388 and NGC 6441 show existence of extended blue tails in HB of high-metallicity clusters (Busso et al. 2007) and canonical stellar evolution theory cannot explain such blue tails (Rich et al. 1997). Castellani & Castellani (1993) have suggested that due to enhanced stellar winds and dynamical interactions within dense (0.6933 pc for NGC6388, 0.5904 pc for NGC 6441; Harris 1996) cluster cores the star looses large amount of envelope mass that fails to ignite helium flash at the RGB tip. So it is forced to move toward the white dwarf cooling sequence. It is still able to ignite at the end of white dwarf cooling sequence, known as early hot flasher (EHF) or along the white dwarf sequence, known as the late hot flasher (LHF). After helium flash the star settles on its ZAHB location. When LHF occurs it occurs under extreme electron degeneracy and it is able to penetrate into the H-rich envelope causing mixing of H into hot He-burning regions where it burns very quickly producing an envelope enriched in He, C, and N via both H and He burning (Sweigart 1997; Brown et al. 2001). So along the HB there is a gap at the hot end of the HB between unmixed (EHF) and mixed (LHF) models. Also numerical simulations (Busso et al. 2007) showed that the He enrichment can be as high as 0.40 and 0.35 to explain the observed blue tails in these metal-rich clusters. So the present AGB model cannot predict extreme helium enhancement (Karakas et al. 2006) which is characteristics of high-metallicity GCs (Caloi & D'Antona 2007; D'Antona et al. 2005; Norris 2004; Piotto et al. 2005) but EHF and LHF model can explain the He abundance to some extent. In Table 7, mean core radius hence central surface brightness and central luminosity density are higher in Cluster 1 (denser environment) compared to Cluster 2. So EHF–LHF model supports the extreme He enrichment according to Castellani & Castellani (1993) rather than AGB model. Several studies (Frank & Gisler 1976; Smith 1996; Gnedin et al. 2002) have suggested that GCs are unlikely to retain AGB ejecta owing to ram pressure stripping by warm/cold gas of Galactic halo and disk. These imply that GCs are unlikely to retain AGB ejecta in protogalactic environment where denser halo/disk gas can strip the AGB ejecta efficiently from GCs during hydrodynamical interactions between the gas and AGB ejecta. In the present situation, the GCs in Cluster 1 are less massive ($\langle M_V \rangle \sim -7.54$, Table 7) compared to GCs of Clusters 2 and 3. So lower cluster potential does not help much to retain AGB ejecta. In a word AGB model has controversy in case of high-metallicity, low-mass, high-density GCs, i.e., for high-metallicity GCs dense environment (i.e., high ρ_0, less r_c) is responsible for producing blue tail of the HB. Our present result (Equation (1)) reflects the same fact for GCs in Cluster 1 which

Table 4
Estimation of Regression Coefficients using Bootstrap Samples for Cluster 1

Parameter	Observed	Bias	Mean	Variance
Intercept	6.0514	1.066×10^{-14}	6.0514	
[Fe/H]	−0.4102	6.66×10^{-16}	−0.4102	$<10^{-14}$
μ_v	−0.1510	4.996×10^{-16}	−0.1510	
r_c	0.1258	-6.016×10^{-16}	0.1258	

Table 5
Estimation of Regression Coefficients using Bootstrap Samples for Cluster 2

Parameter	Observed	Bias	Mean	Variance
Intercept	2.3951	-8.88×10^{-16}	2.3951	
[Fe/H]	−0.3596	1.11×10^{-16}	−0.3596	$<10^{-16}$
M_v	−0.1525	4.44×10^{-16}	−0.1525	

Table 6
Estimation of Regression Coefficients using Bootstrap Samples for Cluster 3

Parameter	Observed	Bias	Mean	Variance
Intercept	3.62812	-2.31×10^{-14}	3.62812	
[Fe/H]	−0.06716	1.80×10^{-16}	−0.06716	$<10^{-14}$
M_v	−0.05686	2.84×10^{-16}	−0.05686	

Table 7
Group Means for the Parameters of the GCs Found by CA of the Present Sample

Parameter	Cluster 1	Cluster 2	Cluster 3
Number of members	24	18	8
[Fe/H]	−1.15	−1.45	−1.69
M_v	−7.54	−8.21	−7.95
c	1.70	1.80	1.27
r_c	1.09	1.30	0.96
R_{gc}	2.92	9.18	22.38
μ_V	16.95	16.60	16.40
ρ_0	4.25	3.88	3.86

are of high metallicity and dense in nature. Also self-pollution model cannot quantitatively produce Na–O, Mg–Al anticorrelations (Fenner et al. 2004). The serious problem is the first one. For this a modified scenario known as "external pollution" has been suggested by Bekki et al. (2007). According to this model GCs are initially more massive than the present-day GCs by a factor of 10–100. These protoglobular clouds are located at the central region of low-mass protogalaxies embedded in the dark matter subhaloes. AGB ejecta of the host galaxy's field stars, which formed earlier and surrounded the clouds, go into star formation within the clouds on a timescale of $\sim 10^7$ yr and the low-mass galaxies were destroyed by the Galactic tidal field to become the halo components, whereas the GCs were tidally stripped to form Galactic halo GCs. In this scenario, there can be very small age differences ($\sim 10^7$ yr) between stars with different abundances in a single GC. This model can explain the large fraction of CN strong stars but cannot explain the Na–O anticorrelation prevalent in the RGB stars.

For the halo part (Clusters 2 and 3) the morphology of HB is further influenced by the presence of massive clusters besides metallicity as concluded by RB06 and the fit is also comparable with them. In Cluster 3 the fit is very poor, so no firm conclusions can be drawn for the outer halo GCs. Further observations are needed for better conclusion. It is to be noted that AGB model successfully explains the chemical anomalies in HB of low-metallicity GCs (here inner halo GCs) suggesting an episodic star formation model which is consistent with the helium enhancement (Carretta et al. 2006, 2007a, 2007b; Gratton et al. 2006). In Equation (2), M_v is the other important parameter besides metallicity. Now M_v represents the total mass of the cluster and the total mass of a cluster has significant influence on HB morphology. D'Antona et al. (2002) found that helium enrichment governs self-pollution and the spread in helium originates from the evolving mass. So self-pollution and hence helium enrichment would be higher in more massive clusters as they can retain the material from ejecta from first-generation stars due to higher cluster potential compared to less massive and more compact clusters. This accentuates the formation of second-generation stars in larger number leading to blue tail of HB.

So from the above discussion it emerges that AGB model can successfully explain the HB morphology in intermediate metallicity GCs (Cluster 2) but it cannot explain many features for the high metallicity, less massive, and high-density GCs and is suggested to be revised.

5. CLUSTER ANALYSIS AND RGB STARS

Carretta et al. (2006, 2007a, 2007b) have studied RGB stars of GGC NGC 2808, 6752, and 6218 and found two generations of stars (He rich and He poor) by observing a jump in O and Na abundances in these two generations. Now the above GGC are classified as the inner halo GCs (Cluster 2, CC07). To find the classification in a more objective way we carried out K-means CA following CC07 with respect to V, $B - V$, [Na/Fe], and [O/Fe] to find the optimum number of coherent groups among the RGB stars in these three GCs. In every situation, the optimum number found is three instead of two as found by Carretta et al (2006, 2007a, 2007b). The group means of the parameters are listed in Table 8. The three subgroups (Clusters I–III) of RGB stars in each GC are also shown in Figure 7. The clustering in CMD for NGC 2808 is not very clear for Cluster III. The red giant bump of NGC 6752 (Data set 3) is at $V = 13.65$ which is very close to Cluster II mean. The red giant bump for NGC 6218 (Data set 4) is at $V = 14.6$ which is in between Cluster II and Cluster III means. A change point analysis (see the Appendix) of NGC 6752 shows that the change points of V magnitudes with respect to color ($B - V$) are at $V = 13.2$ and 14.1. This also reflects a verification of the true nature of the clustering into three groups found by K-means CA as is clear from CMD in Figure 7. The latter change point is almost compatible to the value of red giant bump 13.65. Similar results for change point analysis have been found for other GCs NGC 2808 and 6218 also. These three groups are unlike the two groups found by Carretta et al. (2006a, 2007a, 2007b) by studying the nature of univariate distributions. To verify the evolutionary effect [Na/Fe] (as this is a better measure than [O/Fe]) is plotted against V magnitude for the various groups in the above three GCs (Figure 8). No significant trend is found while the mean values in the groups are clearly different (Table 8). In Table 8, the correlation values between [Na/Fe] and [O/Fe] for Clusters 1–3 are also given for GCs NGC2808, 6752, and 6218. It is apparent from the table that there is wide variation in the cluster sizes for NGC 6752 and 6218 whereas the sizes are more or less comparable for NGC 2808. As a result, for NGC 2808 the increasing trend in the [Na/Fe] mean values are quite prominent and anticorrelation between [Na/Fe] and [O/Fe] also shows an increasing trend. But for NGC 6752 and 6218 this feature is

Table 8
Group Means for the Parameters of RGB Stars found by CA for Different GCs

Globular Cluster	Variables	Cluster I He Poor	Cluster II He Medium	Cluster III He Rich
NGC 2808	Number of members	39	29	26
	V	14.36 ± 0.036	15.13 ± 0.046	14.85 ± 0.083
	B	15.74 ± 0.026	16.35 ± 0.039	16.09 ± 0.064
	[O/Fe]	0.18 ± 0.034	0.31 ± 0.021	−0.5 ± 0.048
	[Na/Fe]	0.17 ± 0.032	0.07 ± 0.026	0.53 ± 0.033
	$B - V$	1.38 ± 0.012	1.22 ± 0.010	1.25 ± 0.019
	[O/Na]	0.02 ± 0.063	0.24 ± 0.040	−1.03 ± 0.069
	r([Na/Fe], [O/Fe])	−0.41	−0.49	−0.82
NGC 6752	Number of members	32	60	45
red giant bump	V	12.49 ± 0.072	13.55 ± 0.027	14.26 ± 0.028
at $V = 13.65$	B	13.49 ± 0.058	14.40 ± 0.024	15.04 ± 0.025
	[O/Fe]	0.18 ± 0.049	0.16 ± 0.032	0.19 ± 0.030
	[Na/Fe]	0.44 ± 0.043	0.38 ± 0.036	0.32 ± 0.036
	$B - V$	1.10 ± 0.014	0.84 ± 0.0035	0.77 ± 0.0036
	[O/Na]	−0.26 ± 0.079	−0.22 ± 0.062	−0.13 ± 0.056
	r([Na/Fe], [O/Fe])	−0.48	−0.66	−0.42
NGC6218	Number of members	9	27	43
red giant bump	V	12.59 ± 0.16	14.10 ± 0.074	15.10 ± 0.051
at $V = 14.6$	B	13.97 ± 0.099	15.14 ± 0.064	16.04 ± 0.047
	[O/Fe]	0.22 ± 0.079	0.032 ± 0.038	0.36 ± 0.039
	[Na/Fe]	0.44 ± 0.11	0.48 ± 0.038	0.16 ± 0.033
	$B - V$	1.39 ± 0.063	1.04 ± 0.010	0.94 ± 0.0047
	[O/Na]	−0.22 ± 0.15	−0.45 ± 0.067	0.20 ± 0.065
	r([Na/Fe], [O/Fe])	−0.25	−0.60	−0.56

not reflected in the mean values whereas the anticorrelations show almost increasing trend for NGC 6218. In case we have a large number of GCs then the above feature is expected to be prominent for all the GCs.

For GGC in Cluster 1, there are some observations of RGB stars of NGC 104 (seven observations; Carretta et al. 2004) and NGC 362 (13 observations; Shetrone & Keane 2000) for which all the values of V, $B-V$, [Na/Fe], [O/Fe] are available. But the sample sizes are very very small for drawing any firm statistical conclusion. Hence, subject to observational limitations it has not become possible to study the properties of RGB stars of GCs belonging to Cluster 1. Therefore, multi-episodic star formation is preferred for AGB stars in halo GGC having intermediate/low metallicity.

6. CONCLUSION

Through the present study, we have extracted some of the new features (as listed below) of HB morphology which can better explain the history of GGCs in a more objective way.

1. Different authors have considered different HB morphology parameters in a subjective way. In the present work, the most significant parameter is selected objectively through PCA considering initially all the parameters discussed by different authors. It is found that $\log T_{\rm eff\,HB}$ is the most significant parameter which takes into account the maximum variation of the HB. Thus, selection of proper HB morphology parameter in an objective way is the new aspect compared to all the subjective ways of selection by previous authors.
2. HBs of different GGC are studied separately in different regions, e.g., bulge/disk, inner halo, and outer halo of the Galaxy instead of considering whole region together. It is found that in the bulge/disk part AGB model cannot successfully explain the high He abundance and retention of AGB ejecta by ram pressure but EHF–LHF model can explain to some extent the extreme He enrichment in high-density (i.e., high ρ_0) and high-metallicity, compact (i.e., low r_c) GCs. In the halo part the GCs are massive ($\langle M_V \rangle \sim -8.21, -7.95$, Table 7). Now massive GCs can retain the material of the ejecta from first-generation stars due to higher cluster potential. This leads to formation of second-generation stars leading to blue tail of the HB. Study of HB morphology in different regions of the Galaxy brings new information for the formation of stars in GGC which is similar to previous work (RB06) in the halo part but is different in the disk part. This is also a new finding of the present work.
3. In the halo part, there are three stellar populations found by CA suggesting a multi-episodic star formation process. This is another new aspect of the present work.
4. For prediction of the HB morphology parameter a different technique (stepwise multiple regression technique) is used instead of ordinary regression which automatically rejects the insignificant parameters and includes only the most significant ones in the regression equation.
5. Also the regression equation found fits very well in case of disk GGC (Equation (1), multiple $R^2 \sim 0.85$) compared to that found in the previous work (multiple $R^2 \sim 0.5276$; Figure 8; RB06) by analyzing all the GGC as a single sample.

One of the author Tanuka Chattopadhyay thanks University Grants Commission for awarding her a Major Research Grant for the work. She also thanks Department of Statistics, Astrostatistics Centre, Pennsylvania State University for providing her a NSF grant. Tanuka Chattopadhyay and Asis Kumar Chattopadhyay are also thankful to IUCAA for assistance

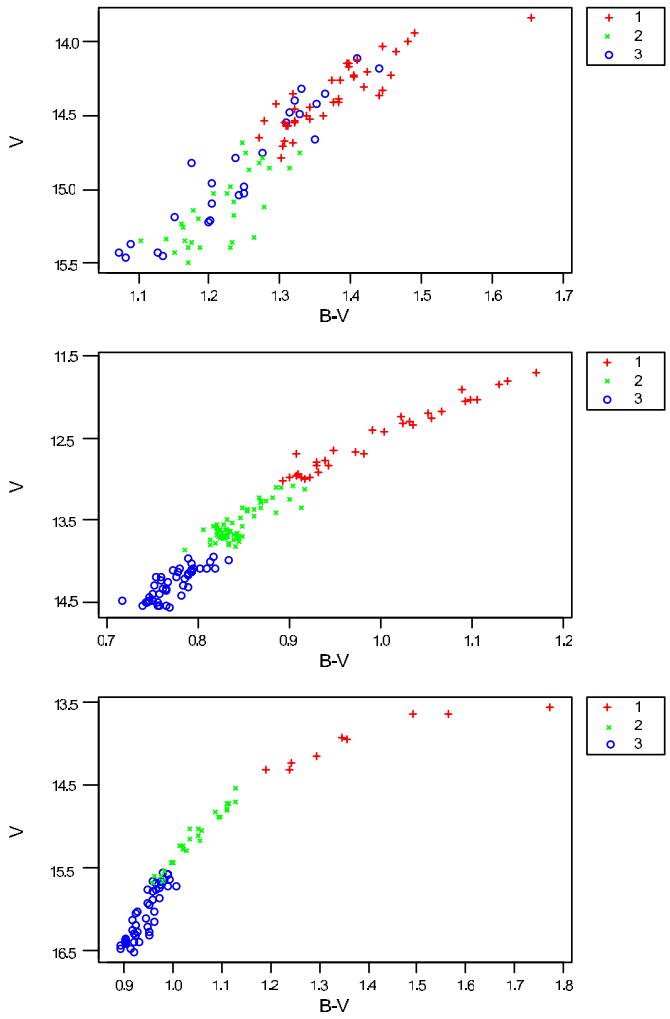

Figure 7. From top to bottom CMD for three groups of GCs found in CA for RGB stars in GCs NGC 2808, 6752, and 6218, respectively.

(A color version of this figure is available in the online journal.)

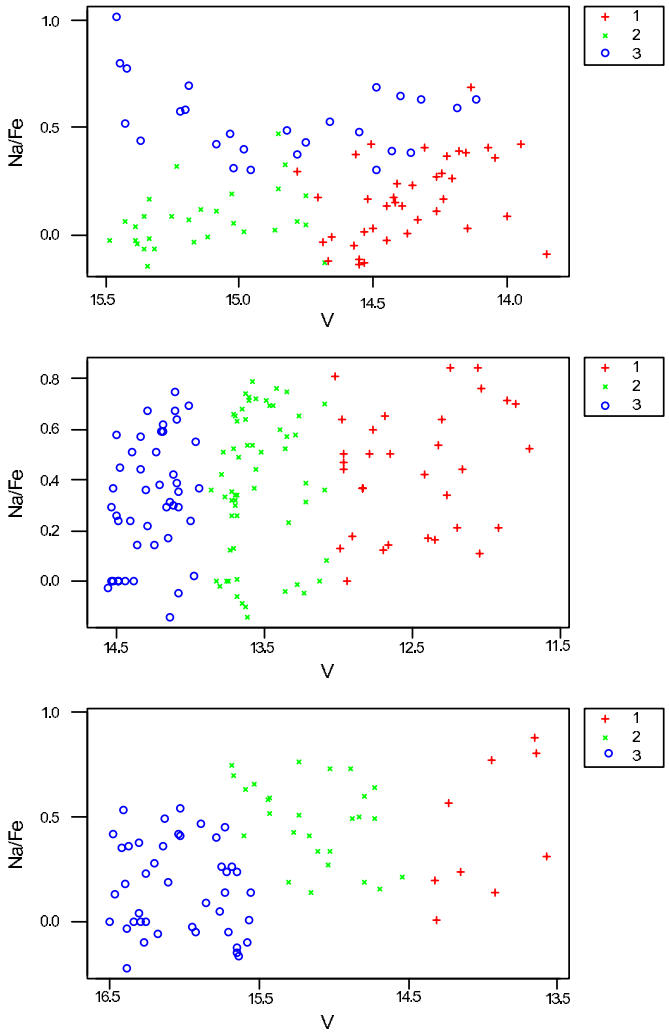

Figure 8. From top to bottom [Na/Fe] vs. *V*-magnitude diagrams for the three groups found in CA for RGB stars of each of the GCs NGC 2808, 6752, and 6218, respectively.

(A color version of this figure is available in the online journal.)

through Associateship Programme. The authors are grateful to the referee Flavio Fusi Pecci for his valuable suggestions to improve the quality of the manuscript.

APPENDIX

PETTITT'S NONPARAMETRIC TEST FOR DETECTION OF CHANGE POINT

The problem may be stated as below.

Consider a sequence of continuous random variables $X_1, X_2, \ldots, X_T$. Let the first τ variables $X_1, \ldots, X_\tau$ have a common distribution function $F_1(x)$ and the next $(T - \tau)$ variables $X_{\tau+1}, \ldots, X_T$ have a common distribution function $F_2(x)$. It is known that $1 \leqslant \tau < T$. The value of the index τ is known as the change point which is unknown. There are several parametric approaches to find out the value of τ. Pettitt (1980) developed the following nonparametric method using the nonparametric statistic suggested by Sen & Srivastava (1975). Here, the null hypothesis is "there is no change point" and the alternative hypothesis is "there is a change point at $\tau (1 \leqslant \tau < T)$." The nonparametric test statistic is given by

$$U_t = \sum_{i=1}^{t} \sum_{j=t+1}^{T} \mathrm{sign}(X_i - X_j),$$

where

$$\begin{aligned} \mathrm{sign}(x) &= -1 \quad \text{if} \quad x < 0, \\ &= \ \ 0 \quad \text{if} \quad x = 0, \\ &= +1 \quad \text{if} \quad x > 0. \end{aligned}$$

If there is no change then $\mathrm{sign}(X_i - X_j)$ has zero mean and thus $U_t\{t(T-t)\sigma^2(s)\}^{-1/2}$ is asymptotically standard normal, where $\sigma^2(s)$ is some normalizing constant independent of t. A nonparametric estimate of τ is given by that value of t which maximizes $U_t^2\{t(T-t)\}^{-1}$ with respect to t.

REFERENCES

Bekki, K., Campbell, S. W., Lattanzio, J. C., & Norris, J. E. 2007, MNRAS, 377, 335
Bolte, M. 1989, AJ, 97, 1688
Brown, T. M., et al. 2001, ApJ, 562, 368
Buonanno, R., et al. 1997, AJ, 113, 706
Busso, G., et al. 2007, A&A, 474, 105
Caloi, V. 2001, A&A, 366, 91
Caloi, V., & D'Antona, F. 2007, A&A, 463, 949
Carretta, E. 1994, PhD thesis, Univ. of Padova
Carretta, E., et al. 2004, A&A, 416, 925
Carretta, E., et al. 2006, A&A, 450, 523

Carretta, E., et al. 2007a, A&A, 464, 927
Carretta, E., et al. 2007b, A&A, 464, 939
Carvalho, R. M. 1999, Ap&SS, 265, 191
Castellani, M., & Castellani, V. 1993, ApJ, 407, 649
Castellani, V., et al. 2006, A&A, 446, 569
Catelan, M., et al. 2002, AJ, 124, 364
Chattopadhyay, T., & Chattopadhyay, A. K. 2006, AJ, 131, 2452
Chattopadhyay, T., & Chattopadhyay, A. K. 2007, A&A, 472, 131
D'Antona, F., & Caloi, V. 2004, ApJ, 611, 871
D'Antona, F., et al. 2003, in ASP Conf. Ser. 296, New Horizons in Globular Cluster Astronomy, ed. G. Piotto et al. (San Francisco, CA: ASP), 293
D'Antona, F., et al. 2005, ApJ, 631, 868
Darlington, R. B. 1968, Psychol. Bull., 69, 161
Denisenkov, P. A., & Denisenkova, S. N. 1989, Astron. Tsir., 1538, 11
Efron, B., Hastie, T., Johnstone, I., & Tibshirani, R. 2004, Ann. Stat., 32, 407
Fenner, Y., et al. 2004, MNRAS, 353, 789
Frank, J., & Gisler, G. 1976, MNRAS, 176, 533
Fusi Pecci, F., et al. 1993, AJ, 105, 1145
Gabriel, K. R. 1971, Biometrika, 5, 453
Gnedin, O. Y., et al. 2002, ApJ, 568, L23
Gratton, R. G., et al. 2001, A&A, 369, 87
Gratton, R. G., et al. 2003, A&A, 404, 187
Gratton, R. G., et al. 2006, A&A, 455, 271
Harris, W. E. 1996, AJ, 112, 1487
Judge, G. G., et al. 1985, The Theory and Practice of Econometrics (New York: Wiley)
Karakas, A., et al. 2006, ApJ, 652, 1240
Langer, G. E., & Hoffman, R. D. 1995, PASP, 107, 1177
Langer, G. E., Hoffman, R., & Sneden, C. 1993, PASP, 105, 301
Lattanzio, J., et al. 2004, Mem. Soc. Astron. Ital., 75, 322
Lee, Y. W. 1990, ApJ, 363, 159
Mackey, A. D., & Gilmore, G. F. 2004, MNRAS, 355, 504
Mackey, A. D., & van den Bergh, S. 2005, MNRAS, 360, 631
MacQueen, J. 1967, in Fifth Berkeley Symp., Vol. 1, Math. Statist. Prob., ed. L. M. Le Cam & J. Neyman (Berkeley, CA: Univ. California Press), 281
Moehler, S., et al. 1999, A&A, 346, L1
Norris, J. E. 2004, ApJ, 612, 25
Pettitt, A. N. 1980, J. Stat. Comput. Simul., 11, 261
Piotto, G., et al. 2005, ApJ, 621, 777
Recio-Blanco, A., et al. 2006, A&A, 452, 875
Reimers, D. 1977, A&A, 57, 395
Rich, R. M., et al. 1997, ApJ, 484, L25
Rood, R. T. 1973, ApJ, 184, 815
Salaris, M., et al. 2004, A&A, 420, 911
Sandage, A., & Wildey, R. 1967, ApJ, 150, 469
Sarajedini, A., Chaboyer, B., & Demarque, P. 1997, PASP, 109, 1321
Sawa, T. 1978, Econometrica, 46, 1273
Sen, A., & Srivastava, M. S. 1975, Ann. Stat., 3, 98
Shetrone, M. D., & Keane, M. J. 2000, AJ, 119, 840
Smith, G. H. 1996, PASP, 108, 176
Soker, N. 1998, AJ, 116, 1308
Stetson, P. B., van den Bergh, S., & Bolte, M. 1996, PASP, 108, 560
Sugar, A. S., & James, G. M. 2003, J. Am. Stat. Assoc., 98, 750
Sweigart, A. V. 1997, ApJ, 474, L23
Tibshirani, R. 1996, J. R. Stat. Soc. Ser. B, 58, 267
Ventura, P., & D'Antona, F. 2005, A&A, 431, 279
Zinn, R. J. 1986, in Stellar Populations, ed. C. A. Norman, A. Renzini, & M. Tosi (Cambridge: Cambridge Univ. Press), 73
Zinn, R. J. 1993, in Globular Cluster Galaxy Connection, ed. G. H. Smith & J. P. Brodie (San Francisco, CA: ASP), 38